Electronic Supplementary Material (ESI) for ChemComm.

Supporting Information

A single-molecular twin rotor: correlated motion of two pyrimidine rings coordinated to copper

Yusuke Takara,[a] Tetsuro Kusamoto,[a] Tatsuya Masui,[a] Michihiro Nishikawa,[a,b] Shoko Kume[a,c] and Hiroshi Nishihara*[a]

Physical measurements

NMR, ESI-TOF MS

^{1}H NMR spectra were recorded with a Bruker DRX500 spectrometer. ESI-TOF mass spectra were recorded using a Micromass LCT spectrometer. In VT ^{1}H NMR experiments, the sample tube was introduced into the machine cooled to 203 K, and the data was acquired during the heating process.

Cyclic voltammetry

Cyclic voltammograms was recorded with ALS 750A electrochemical analyzers (BAS. Co., Ltd.). The working electrode was a 0.3 mm o.d. glassy carbon, a platinum wire served as the auxiliary electrode, and the reference electrode was an Ag^+/Ag electrode (a silver wire immersed in 0.1 M Bu_4NClO_4/0.01 M $AgClO_4$/CH_3CN). The solutions were deoxygenated with pure argon before measurement. Cyclic voltammograms of **1·PF$_6$** were simulated with the BASi Digisim 3.03a software.

Materials

Tetra-*n*-butylammonium hexafluoro phosphate (purchased from Tokyo Chemical Industry) was recrystallized from HPLC-grade ethanol and dried under vacuum for 24 h. 2,9-Bis(9-anthracenyl)-1,10-phenanthroline (L_{Anth2})[10], 4,4'-dimethyl-2,2'-bipyrimidine (Me_2bipym)[9] were prepared according to literature methods. Other chemicals were used as purchased.

Synthesis of $[Cu(Me_2bipym)(L_{Anth2})]PF_6$

2,9-bis(9-anthracenyl)-1,10-phenanthroline (L_{Anth2}, 49.1 mg, 92.2 μmol) and $[Cu(CH_3CN)_4]PF_6$ (34.6 mg, 94.8 μmol) were stirred for 40 min in dichloromethane (4 ml) under nitrogen atmosphere. 4,4'-dimethyl-2,2'-bipyrimidine (Me_2bipym, 20 mg, 58 μmol) was added to the resulted orange solution, and the solution immediately changed to deep red. After filtration, diethyl ether was added to the filtrate to precipitate **1·PF$_6$** as a deep red solid. Yield: 17 mg (20 %).

^{1}H NMR (500 MHz, $(CD_3)_2CO$, 253 K) δ 9.31 (d, J = 8.1 Hz, phen, *ii*), 9.27 (d, J = 8.1 Hz, phen, *io*), 9.25 (d, J = 8.1 Hz, phen, *oo*), 8.68 (s, phen, *ii*), 8.66 (s, phen, *io*), 8.64 (s, phen, *oo*), 8.54 (d, J = 8.1 Hz, phen, *ii*), 8.46 (d, J = 8.1 Hz, phen, *io*), 8.44 (d, J = 8.1 Hz, phen, *oo*), 8.40 (d, J = 4.8 Hz, bpym, *ii*), 8.28 (d, J = 4.9 Hz, bpym, *io*), 8.04 (s, Anth, *io*), 8.03 (s, Anth, *oo*), 8.01 (s, Anth, *ii*), 7.63-7.60 (m), 7.40 (d, J = 8.7 Hz, Anth), 7.37 (d, J = 8.7 Hz, Anth), 7.32-7.29 (m), 7.25 (d, J = 5.3 Hz, bpym, *io*), 7.22-7.09 (m), 6.77 (d, J = 4.8 Hz, bpym, *ii*), 6.66 (d, J = 4.9 Hz, bpym, *io*), 6.54 (d, J = 5.3 Hz, bpym, *io*), 6.45 (d, J = 5.3 Hz, bpym, *oo*), 2.41 (s, Me, *o*), 2.37 (s, Me, *io*), 1.57 (s, Me, *io*), 1.50 (s, Me, *ii*).

ESI-TOF-MS *m/z* 781.2144 (calcd. for $[M\text{-}PF_6]^+$, 781.2141)

Table S1 Fitting parameters of the ring inversion processes for **1·PF$_6$** in 0.1 M ^{n}Bu$_4$NPF$_6$-acetone

	293 K	273 K	253 K	219 K
E_{oo} / V	0.265	0.22	0.185	0.14
E_{io} / V	0.48	0.449	0.425	0.375
E_{ii} / V	0.61	0.584	0.57	0.53
K^{I}*ii→io*	2.6	2.5	2.2	2
K^{I}*io→oo*	0.2	0.18	0.17	0.14
K^{II}*ii→io*	4.5×10^{2}	7.7×10^{2}	1.3×10^{3}	7.3×10^{3}
K^{II}*io→oo*	9.9×10^{2}	3.1×10^{3}	1.1×10^{4}	3.6×10^{4}
$k^{I}_{ii\rightarrow io}$ / s^{-1}	11	1.3	0.1	0
$k^{I}_{io\rightarrow oo}$ / s^{-1}	8	2.7	0.5	0
$k^{I}_{oo\rightarrow io}$ / s^{-1}	40	15	3	0
$k^{I}_{io\rightarrow ii}$ / s^{-1}	4	0.5	0.05	0
$k^{II}_{ii\rightarrow io}$ / s^{-1}	3.2	1.5	6.4×10^{-1}	0
$k^{II}_{io\rightarrow oo}$ / s^{-1}	5.0	3.1	1.1	0
$k^{II}_{oo\rightarrow io}$ / s^{-1}	5.0×10^{-3}	1.0×10^{-3}	1.0×10^{-4}	0
$k^{II}_{io\rightarrow ii}$ / s^{-1}	7.0×10^{-3}	2.0×10^{-3}	5.0×10^{-4}	0
α_{oo}	0.5	0.5	0.3	0.5
α_{io}	0.5	0.5	0.5	0.35
α_{ii}	0.5	0.5	0.5	0.35
R_u	700	800	1000	1600
C_{dl} / F	4.2×10^{-6}	4.2×10^{-6}	4.2×10^{-6}	3.0×10^{-6}
D / cm^2 s^{-1}	1.2×10^{-5}	8.5×10^{-6}	4.5×10^{-6}	2.0×10^{-6}

Table S2 Thermodynamic and kinetic parameters of **1·PF$_6$** in 0.1 M ^{n}Bu$_4$NPF$_6$-acetone

	ii→*io*	*io*→*oo*	*oo*→*io*	*io*→*ii*
ΔH /kj mol^{-1}	2.0	2.4	-2.4	-2.0
ΔS /j K^{-1} mol^{-1}	15	-5.4	5.4	-15
ΔG°/kj mol^{-1}	-2.4	4.0	-4.0	2.4
$\Delta H^{\neq}$/kj mol^{-1}	68	41	38	65
$\Delta S^{\neq}$/j K^{-1} mol^{-1}	6.4	-88	-84	-11
$\Delta G^{\neq}$/kj mol^{-1}	66	67	63	68

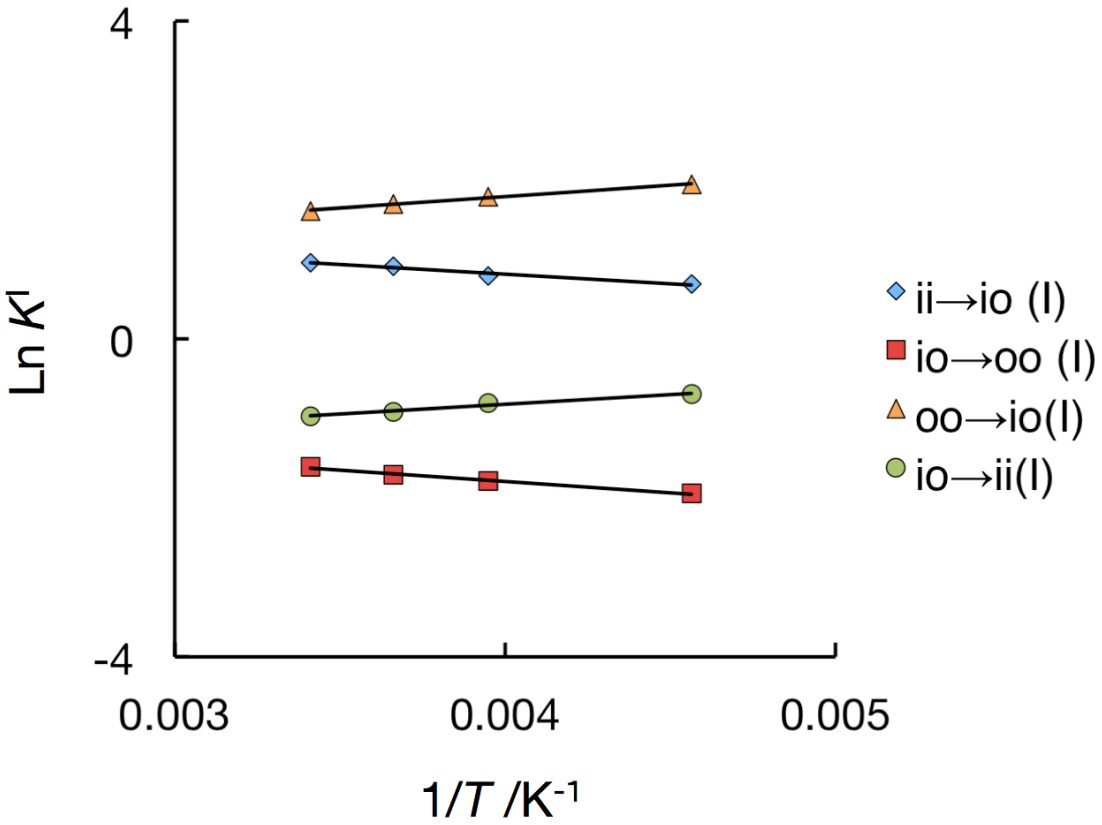

Fig. S1 van't Hoff plots of **1·PF$_6$** obtained by simulative analysis on cyclic voltammograms.

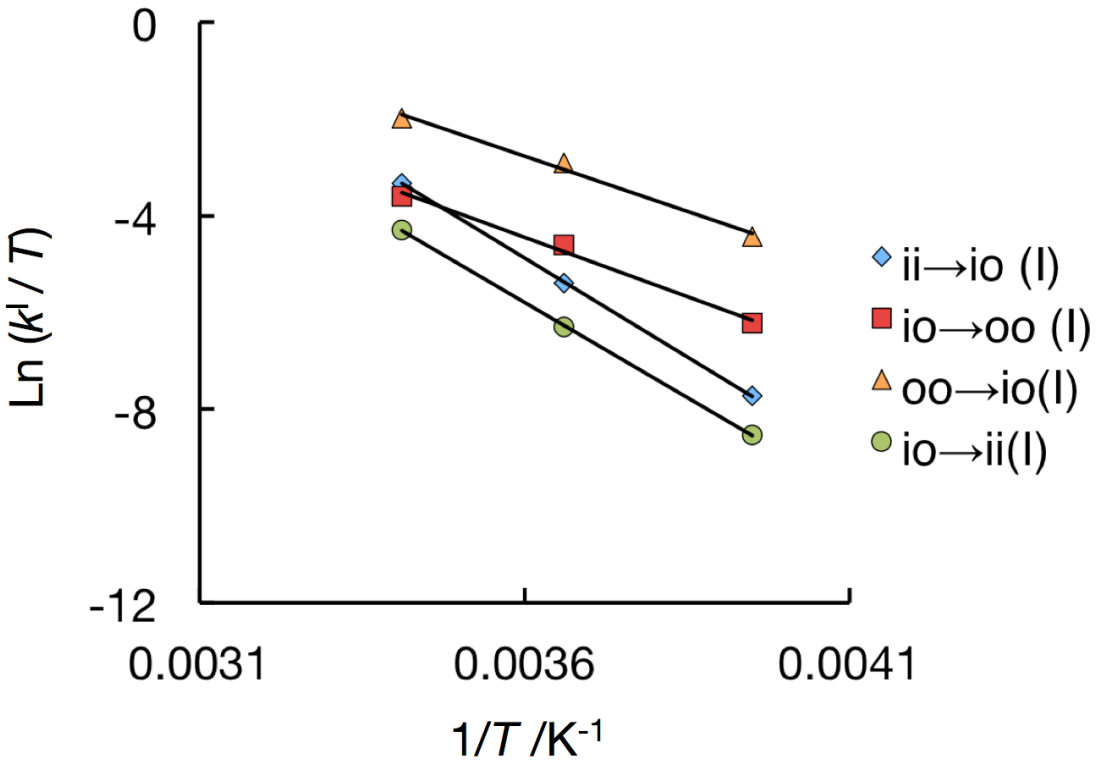

Fig. S2 Eyring plots of **1·PF$_6$** obtained by simulative analysis on cyclic voltammograms.

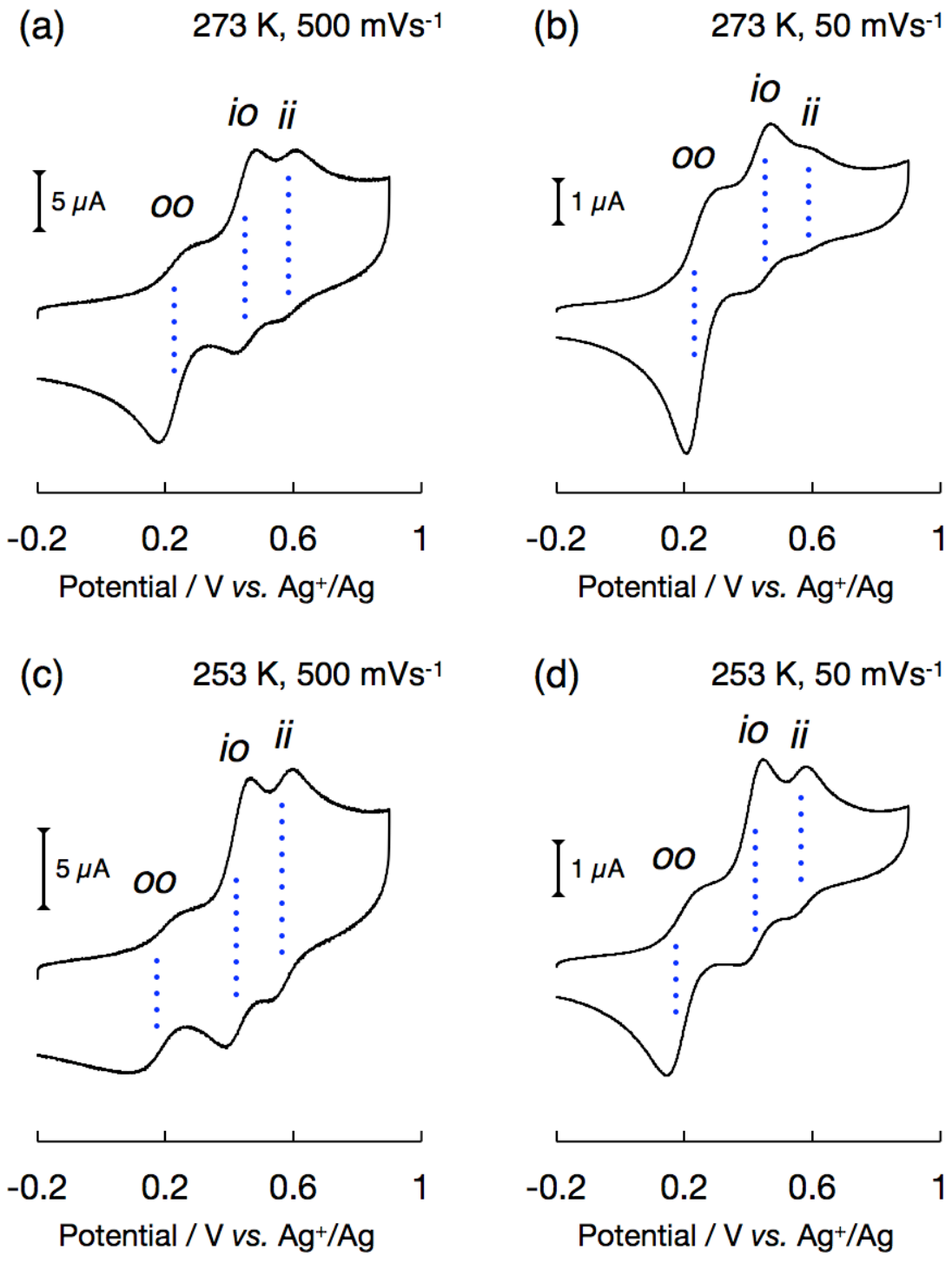

Fig. S3 Cyclic voltammograms of $\mathbf{1}^{+}$ (0.5 mM) in 0.1 M $^{n}Bu_4NPF_6$-acetone at various temperatures and scan rates. (a) 273 K and 500 mVs^{-1}, (b) 273 K and 50 mVs^{-1}, (c) 253 K and 500 mVs^{-1}, and (d) 253 K and 50 mVs^{-1}. All voltammograms are for the first cycle.

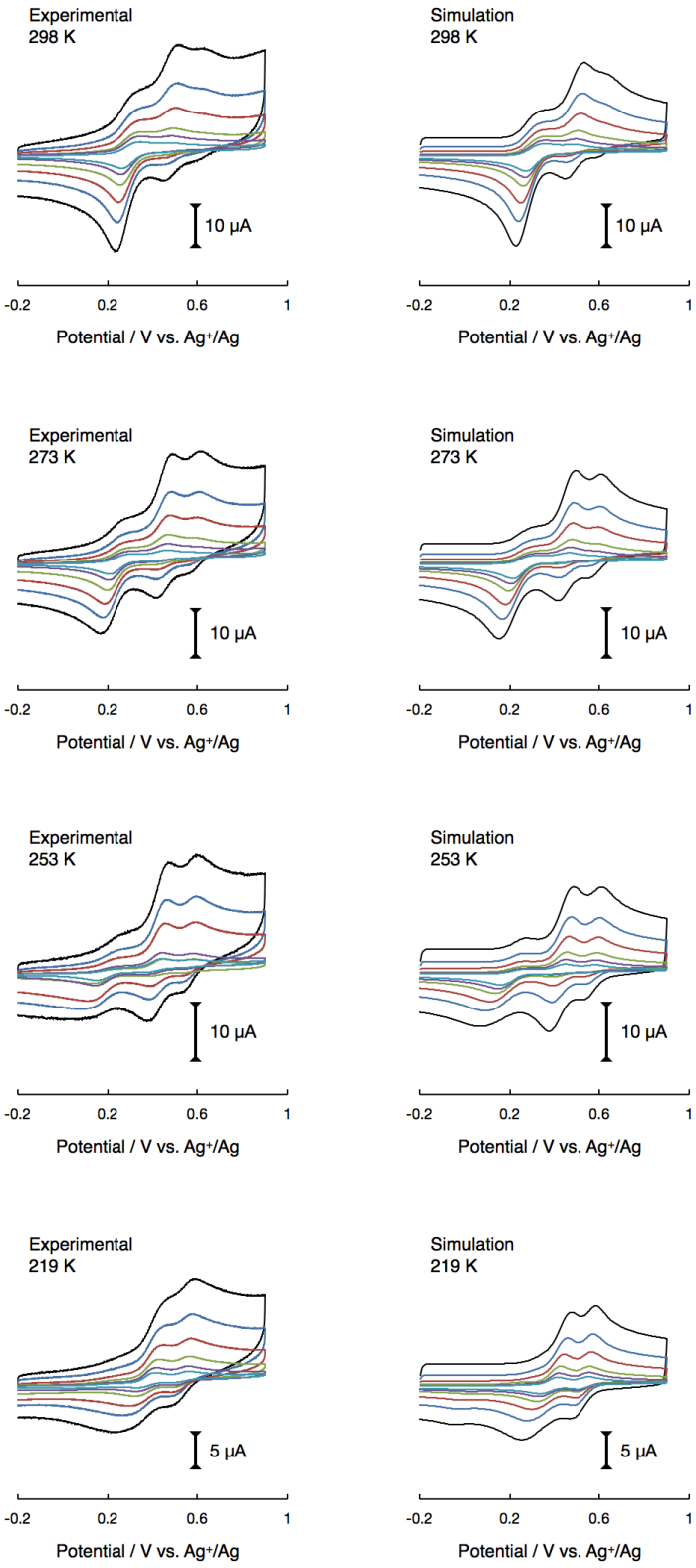

Fig. S4 Experimental and simulated cyclic voltammograms of $\mathbf{1}^{+}$ (0.5 mM) in 0.1 M $^{n}Bu_4NPF_6$-acetone at various temperatures and scan rates (1000, 500, 250,100, 50, 25 mVs^{-1}). All voltammograms are for the first cycle.

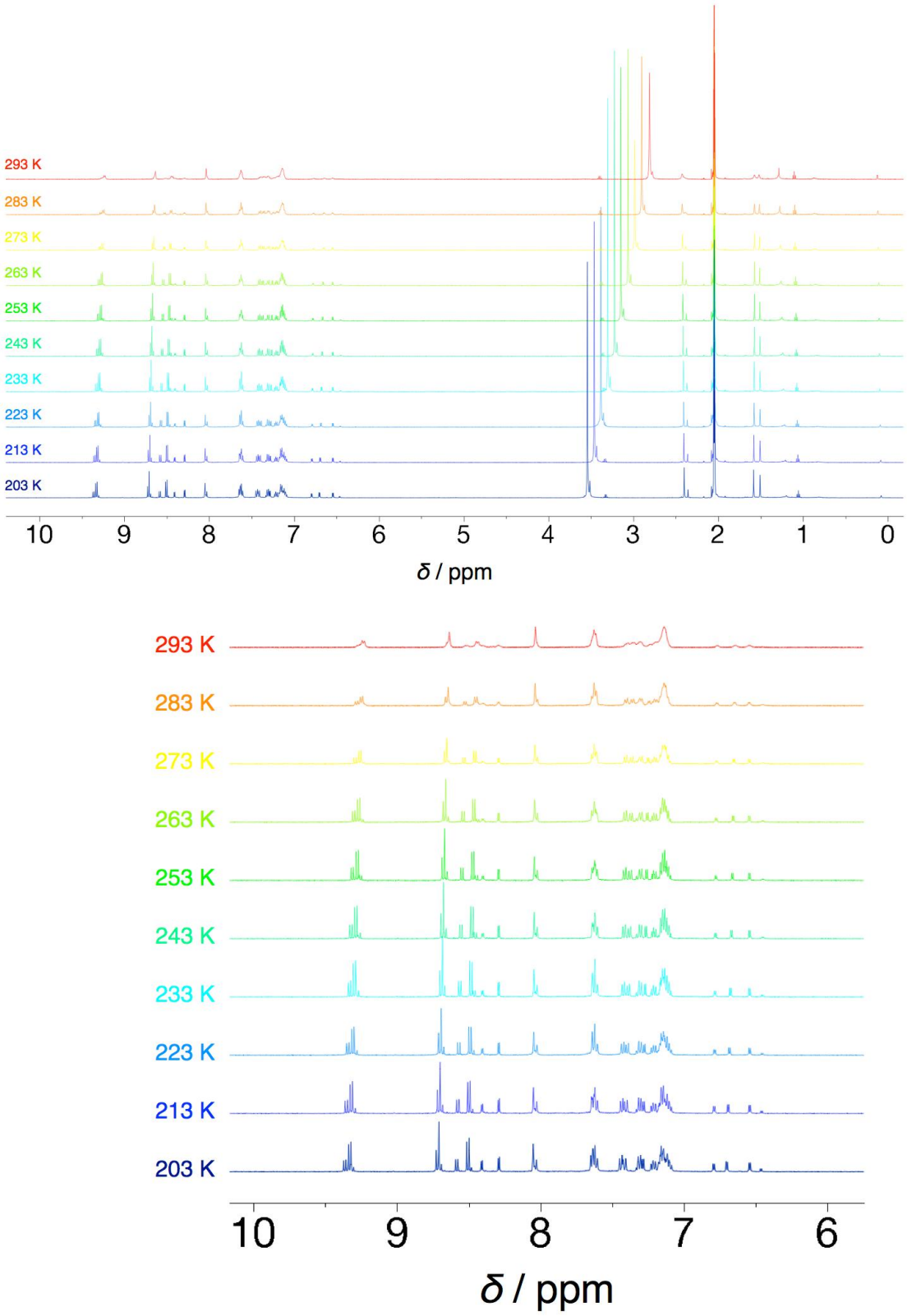

Fig. S5 ^{1}H NMR spectra of **1·PF$_6$** in acetone-d_6 at various temperatures.

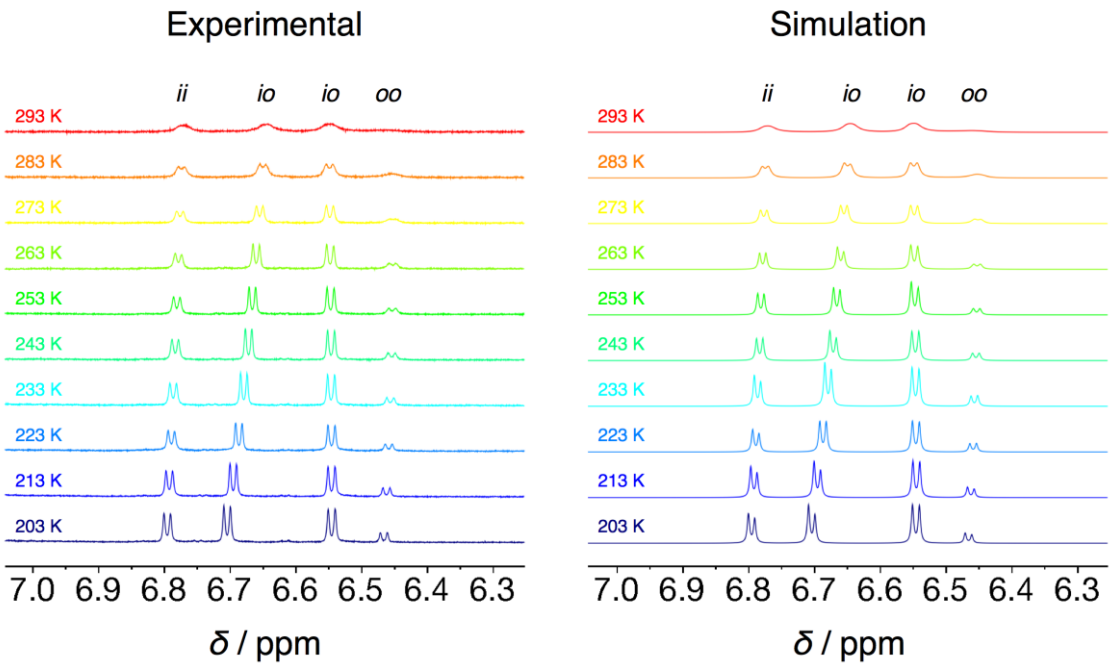

Fig. S6 Experimental and simulated ^{1}H NMR spectra of **1·PF$_6$** in acetone-d_6 at various temperatures.

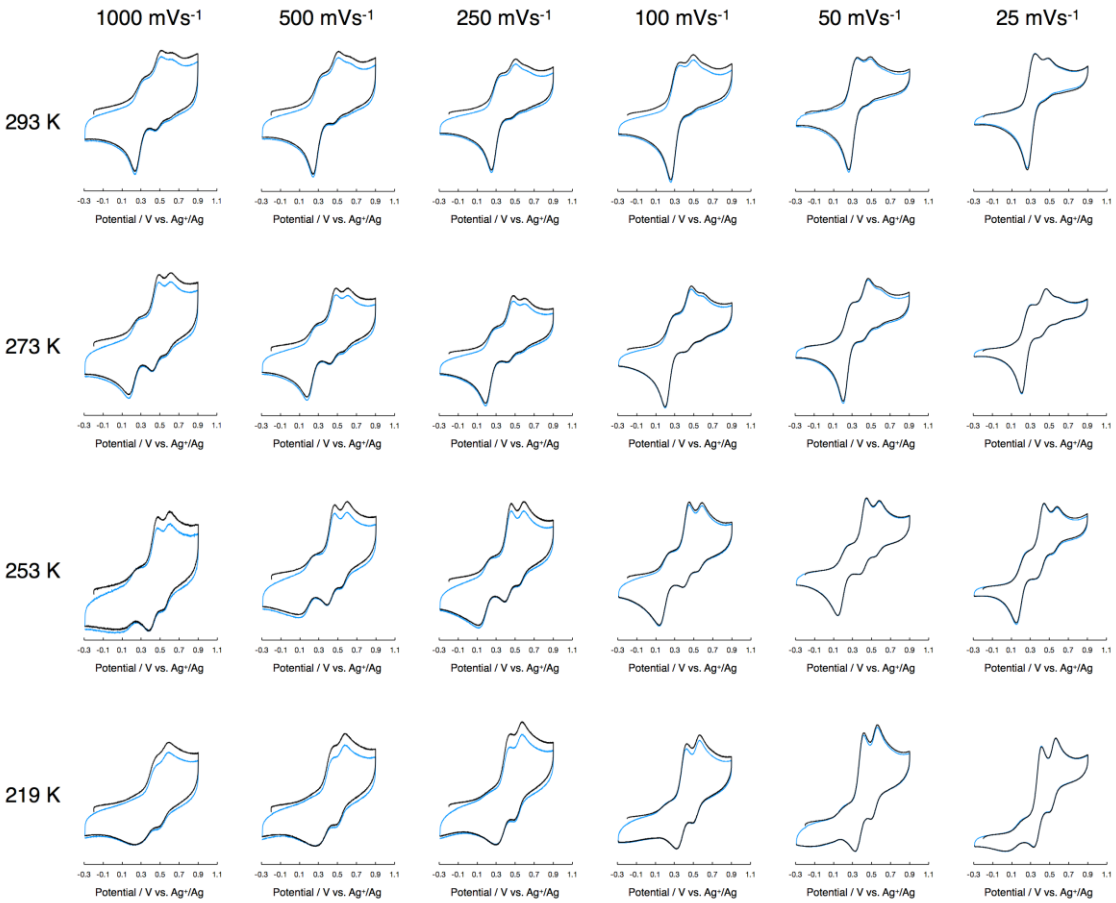

Fig. S7 Cyclic voltammograms of $\mathbf{1}^{+}$ (0.5 mM) in 0.1 M $^{n}Bu_4NPF_6$-acetone at various temperatures and scan rates. Black and blue curves are for the 1st and 2nd potential cycles, respectively.

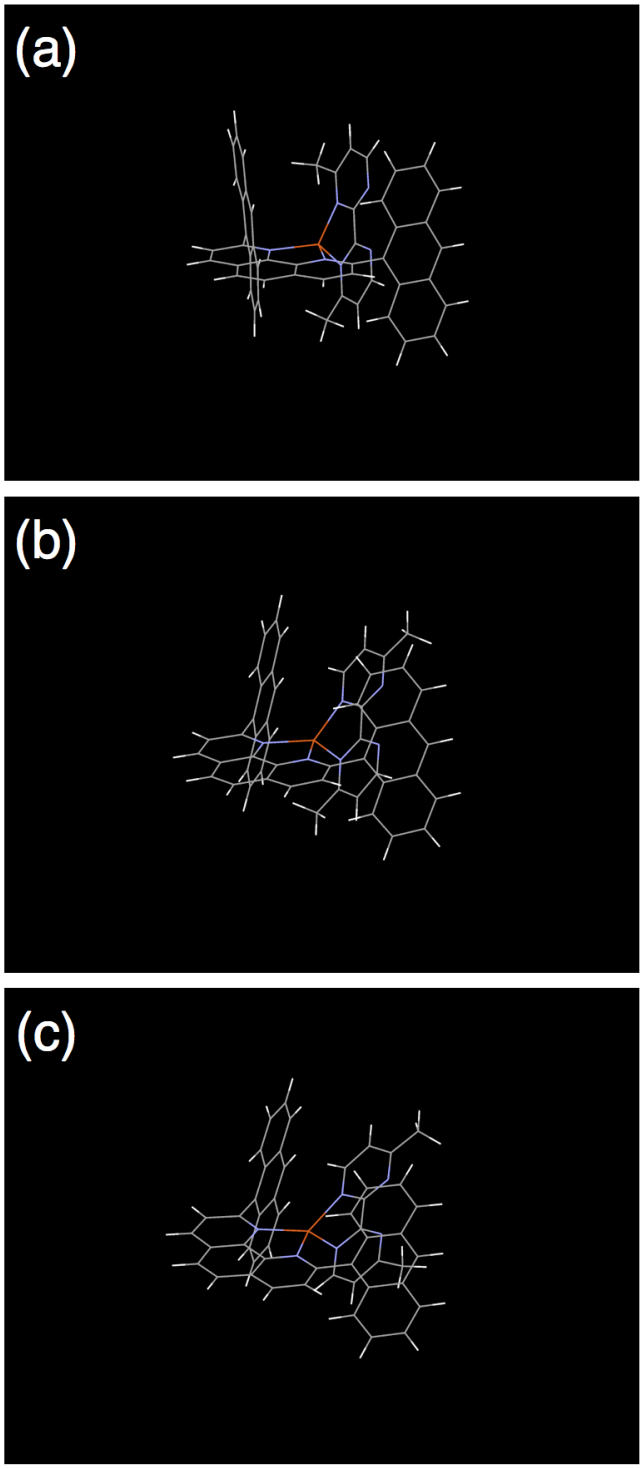

Fig. S8 Optimized structures (B3LYP/LANL2DZ for Cu, /6-31g(d) for the other atoms) of *ii*-isomer (a), *io*-isomer (b) and *oo*-isomer (c).

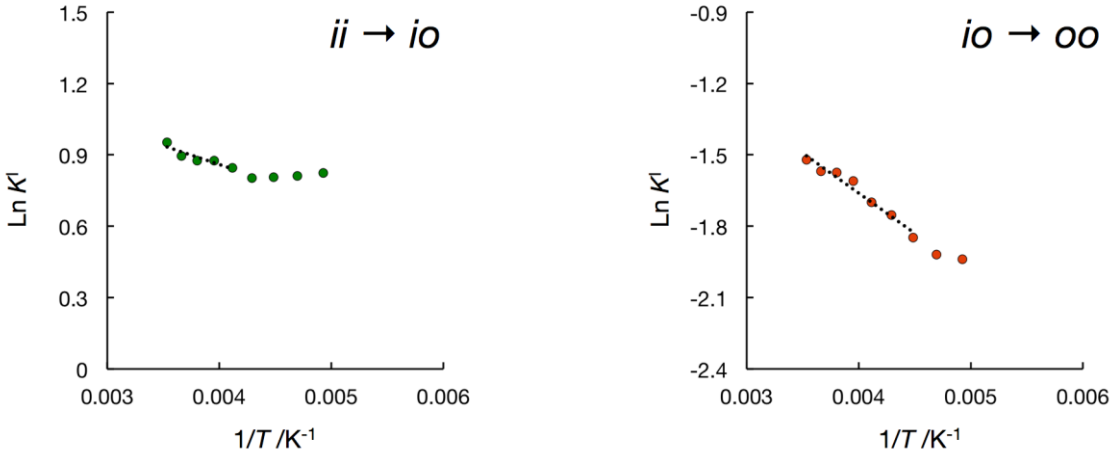

Fig. S9 van't Hoff plots obtained from the integrated values of the ^{1}H NMR signals in acetone-d_6.